

Inorganic particle toughening II: toughening mechanisms of glass bead filled epoxies

J. Lee¹, A.F. Yee*

Macromolecular Science and Engineering Program, The University of Michigan, Ann Arbor, MI 48109, USA

Received 29 February 2000; received in revised form 16 May 2000; accepted 16 May 2000

Abstract

Based on the previously established knowledge about the micro-mechanical deformations occurring during the fracture of glass bead filled epoxies, the major energy dissipation mechanisms are investigated. Correlation studies between the fracture toughness of composites and the size of micro-mechanical deformation zones (or areal density of deformation) are used to assess the contributions of the deformations to toughening. Among the deformations found in the fracture of glass bead filled epoxies, i.e. micro-shear banding, debonding of glass beads/diffuse matrix shear yielding, and step formation, micro-shear banding is established as the major and most effective toughening mechanism. In terms of this mechanism, the negligible effect of surface treatments of glass beads on the fracture toughness of glass bead/thermoset composites can be explained successfully. This mechanism is expected to give more detailed and fundamental understanding of inorganic particle toughening than the crack front bowing mechanism. © 2000 Published by Elsevier Science Ltd.

Keywords: Epoxy; Fracture; Toughening

1. Introduction

Numerous previous studies [1–6] have shown that the toughening of thermosets using inorganic particles has some rather complicated aspects. Consequently, it seems improbable that a simple mechanism can explain all the observed fracture behavior. Despite this reservation, in most publications [1–7], the crack front bowing (or crack front pinning) mechanism is considered the major toughening mechanism for inorganic particle toughening. Indeed, this theory can offer simple and satisfying predictions about the effect of particle volume fraction. However, as can be expected, many of the complicated aspects have never been explained successfully by this theory.

The crack front bowing mechanism was first proposed by Lange [8]. To explain the toughening effect from the incorporation of rigid particles into brittle matrices, he used the ‘line tension concept’ that had been developed in studies on dislocation motion in ceramic materials. According to this mechanism, when a crack propagates in a rigid particle filled composite, the rigid particles will resist it. Because of this resistance, the primary crack front has to bend

between particles (bowing). The bowed secondary crack front has more elastic energy stored than the straight unbowed crack front. Therefore, more energy is needed for a crack to propagate. Lange derived a simple equation based on this line tension concept [8]:

$$G_c = 2(G_m^0 + 2T/D_i) \quad (1)$$

where G_c is the fracture energy of the composite, G_m^0 the fracture energy of the matrix, T the line energy per unit length of crack, and D_i the inter-particle separation.

Lange observed experimentally the crack front bowing in the fracture of magnesium oxide crystals containing small voids [8]. Because of the mismatch between two planes of crack propagation divided by a particle, the bowed secondary crack fronts leave characteristic step structures behind particles, also known as characteristic tails. This tail structure is often regarded as evidence for the action of the crack front bowing mechanism [2,3,5,8–11]. However, it is not definitely evident because any source that can divide the plane of crack propagation will cause similar step formation without crack front bowing.

In subsequent studies, Lange [5,12,13] introduced an adjustable parameter to modify Eq. (1) to predict the significance of the size effect on toughening at the same inter-particle spacing. His modification was improved by Evans [14], Green et al. [9–11] and Rice et al. [15–17]. Under the

* Corresponding author. Fax: +1-734-763-4788.

E-mail address: afyee@engin.umich.edu (A.F. Yee).

¹ Present address: Department of Chemical Engineering and Materials Science, The University of Minnesota, Minneapolis, MN 55455, USA.

same line tension concept developed by Lange, Evans and Rice et al. expanded the line energy calculations for various particle configurations. Evans calculated the line energy from the ratio of the stress for propagation of the secondary bowed cracks and the stress for the propagation of the primary straight crack without obstacles. These calculations explain the dependence of fracture toughness on the interparticle separation, the size of particles, the shape of bowed secondary cracks (semicircular or semi-elliptical), and the interaction between secondary cracks. Although particles were considered as impenetrable obstacles in these analyses, Evans noted the importance of the impenetrability of particles [14]. Thus, he proposed the use of a parameter, ε_0 ('impenetrability factor') [14]. Green et al. [9–11] suggested that the impenetrability of particles might depend on various factors: size, volume fraction, and fracture toughness of the particles, interfacial strength, coefficients of thermal expansion (CTE) and elastic modulus mismatch [9–11,14]. However, its dependence could not be predicted by the crack front bowing mechanism.

Using the modified theory of Green et al. [9–11], Spanoudakis and Young [2,3] made reasonable predictions for the fracture toughness of glass bead filled epoxies. The theoretical prediction of toughness increase with increasing volume fraction of glass beads agrees well with the experimental data except for high-volume content regions [2,3]. They believed that the degree of debonding related to the penetrability of particles, and so more glass beads debonded as the volume fraction of glass beads increased, resulting in less effective crack front bowing. However, the independence of fracture toughness on the surface treatments of glass beads, which was found in their study, could not be explained. In addition to the crack front bowing mechanism, the crack-tip blunting mechanism was offered as another underlying mechanism for glass bead filled epoxies, because the strain rate dependence of the fracture toughness could not be understood by using the crack front bowing mechanism. However, neither direct evidence nor details of this crack-tip blunting mechanism was provided in their studies.

According to the modified crack front bowing theories, the line energy or the stress for crack extension depends on the ratio of particle size and inter-particle spacing, where this ratio is a function of particle volume fraction. Thus, the line tension, the volume fraction of particles, and the size of particles can be interrelated successfully. However, the quantitative predictions of this theory cannot consider the effect of interfacial strength, matrix ductility, temperature, strain rate and other materials variables. As an example, an increase in interfacial strength could be expected to improve the impenetrability of particles, resulting in an increase in fracture toughness if cracks propagate along the particle–matrix interface. However, in most studies, the fracture toughness of glass bead filled epoxies does not show any significant dependence on interfacial strength, and in some cases, the fracture toughness increases slightly with the decrease of interfacial strength [2,3].

As a whole, the crack front bowing theory is able to explain the crack propagation and the macroscopic fracture toughness of inhomogeneous materials, if the local fluctuation of fracture toughness in materials (or impenetrability of particles) is known. In this theory, the local fluctuation of fracture toughness is not explained in detail, but assumed as a starting point for the line tension analysis. Therefore, the theory cannot be used for identifying and controlling the origin of the local fluctuation of fracture toughness, which is more important in developing future composite materials. In fact, the impenetrability of particles seems to be a function of various parameters, instead of a simple function of interfacial strength.

Only a few toughening mechanisms other than crack front bowing have been suggested for inorganic particle toughening. Rose [18] argued that the line tension concept is not an appropriate description for toughening by rigid inclusions in brittle matrices. He developed his own crack front interaction model based on the premise that the particles exert a spring-like closure force on two crack surfaces. Several adjustable parameters were used, many of which are somewhat difficult to precisely quantify. The agreement between prediction and experiment, which he found should be treated with caution given the many adjustable parameters involved. Brown [19] suggested enhanced matrix shear yielding as an important mechanism, because he found the similar temperature dependence of fracture toughness as that in rubber particle filled thermosets. However, no evidence of shear yielding was provided. Nakamura et al. [20–25] focused on crack deflection behavior to explain the effect of particle size on the fracture toughness of silica filled epoxies. They found a small but significant increase of fracture toughness with increasing particle size. They believed that larger particles are more effective tougheners, because the larger particles can make the crack propagation path more meandering. Nonetheless, the size effect is not large enough to warrant accepting this proposed mechanism as the major toughening mechanism. Furthermore, the theoretical consideration of the crack deflection toughening mechanism [26] predicts no particle size effect on the toughness of composites.

Recently, Azimi et al. [27] argued that microcracking could be an important mechanism for toughening in glass microballoon filled epoxies. More supportive evidence may be required before the micro-cracking mechanism [28–31] can be considered as the major mechanism instead of the crack front bowing mechanism.

As mentioned previously, although the crack front bowing mechanism has been treated as the major toughening mechanism in inorganic particle filled thermosets, there are many experimental results, which cannot be explained using this mechanism. Therefore, it is clear that further investigation is needed to arrive at a complete explanation for the toughness increase in inorganic particle filled thermosets. In the current experiment, the possible energy dissipating mechanisms are investigated to obtain more

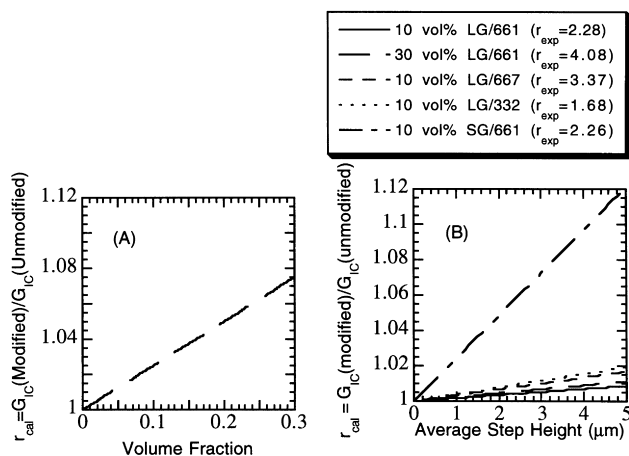


Fig. 1. Toughening effect due to fracture surface increase: (A) fracture energy increase due to the debonding of glass beads versus the volume fraction of glass beads; (B) fracture energy increase due to step formation versus average step height. The r_{exp} value in the parentheses is measured and the r_{cal} (y-axis) is calculated toughness increase.

fundamental understanding than the crack front bowing mechanism, which can disclose the origin of impenetrability (local fluctuation of fracture toughness in materials). In particular, the sizes of micro-mechanical deformation zones where the mechanisms are active are quantified and correlation studies between the sizes and the fracture toughness of composites are performed. From these approaches, micro-shear banding is identified as the major energy dissipating mechanism for glass bead filled epoxies. Cumulative experimental results on the fracture behavior of glass bead filled epoxies are explained in terms of this mechanism. Finally, the applicability and limitations of the crack front bowing mechanism are reexamined in the light of our studies.

2. Experimental

The same glass bead filled epoxies as used in the previous studies [32–35] were used again in this experiment. Glass beads of two different sizes were used and named LG (mean diameter = 24.4 μm) and SG (mean diameter = 3.3 μm). All glass beads were cleaned using distilled water [32–35]. When they are not cleaned, ‘u-’ precedes the designations of glass beads, e.g. u-LG. When the designations of glass beads have numbers, e.g. 0.5-LG, it indicates the feed fraction (%) of rubbery materials (CDI adduct [32–35]), which form an interlayer around glass beads. The t/r (thickness of interlayer/mean radius of glass beads) ratios were found to be 0.55, 1.54, and 2.28% for the feed fraction of 0.5, 1.5, and 3%, respectively [32–35]. Details of cleaning process and rubber encapsulation of glass beads are available elsewhere [32–35]. Four different epoxy matrices, 332, 661, 664, and 667, were used, which were DER 332[®], DER 661[®], DER 664[®], and DER 667[®] (Dow Chemical Co.)

cured by 4,4'-diaminodiphenylsulphone (DDS), respectively.

Debonding zone (region containing debonded glass beads) size was measured using both optical microscopy (OM) and scanning electron microscopy (SEM) of the middle portions of a fracture surface. A total of 15 repeated measurements on more than three fractured SEN-3PB (single-edge-notched three-point bend) [32–35] specimens were averaged for each debonding zone size. Micro-shear (MS) band zone size was measured by using OM micrographs of thin sections of SEN-3PB and DEN-4PB (double-edge-notched four-point bend) [32–35] specimens. The area of MS band zone encompassing all MS bands at the crack tip region was first measured, and the equivalent radius of MS band zone ($2r_{MS}$) was then calculated assuming this zone to be circular. The equivalent radius data can be compared readily with theoretical predictions. The areal density of steps was measured by using digitized SEM images. Regions larger than $10^4 \mu\text{m}^2$ in the process zones of fractured SEN-3PB specimens were selected and digitized. The lengths of steps were then measured by counting the number of pixels along the steps.

The critical strain, defined as the point where tangential modulus drops to 80% of initial modulus, $e_{0.8E}$, was measured by using the uniaxial tensile test data [32–35]. Measuring this strain qualitatively assesses the interfacial strength between glass beads and matrix. Stress–strain curves were smoothed and differentiated, and the measurements of $e_{0.8E}$ by using the differentiated data follows. More than 5 different stress–strain curves were used to obtain an average $e_{0.8E}$ value.

3. Results and discussion

The various micro-mechanical deformations found in glass bead filled epoxies [32–35] can be categorized into three possible energy absorbing mechanisms which are the candidates for the major toughening mechanism: 1. step formation; 2. debonding of glass beads/diffuse matrix shear (DS) yielding; 3. micro-shear (MS) banding. In the following sections, each mechanism is discussed in detail to discover the major toughening source for glass bead filled epoxies.

3.1. Step formation

Step formation may increase fracture energy, because it can increase actual fracture surface area. The mixed mode crack propagation involved in step formation can further increase the fracture toughness of materials. Under the assumption that local crack propagation was always in mode I, the maximum increase of toughness due to the mode II stress component was calculated to be approximately $\sqrt{32}K_{IC}$ [36]. Although this pure mode II stress condition is unlikely to happen in reality, it is true that mixed mode fracture toughness is usually higher than pure

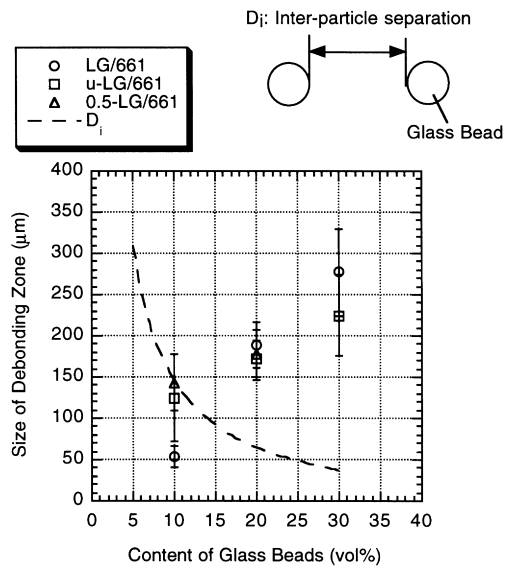


Fig. 2. Debonding zone size ($2r_{dc}$) in SEN-3PB specimens of glass bead filled epoxies measured by optical microscopy on fracture surface. Theoretical inter-particle distance (D_i) is also plotted for comparison.

mode I fracture toughness [36]. A mixed mode stress condition in step formation can also enhance plastic deformation around the step, resulting in the further increase in fracture toughness.

Fig. 1(A) shows the calculated toughness increase (r_{cal}) from the increase of actual fracture surface area by debonding of glass beads. In this calculation, the critical strain energy release rate (G_{IC}) of unmodified epoxy was used as the energy to generate a new unit fracture surface, so the increased fracture surface considered in this calculation is of debonded matrix (fracture surface of the epoxy matrix facing debonded glass beads), not of debonded glass beads. Within the composition range investigated in the plot, the maximum calculated toughness increase is only less than 8%. This is significantly lower than the measured toughness increases (r_{exp}) [32–36]. Clearly, the increase of surface area by debonding is not an important mechanism for glass bead filled epoxies.

Among the various types of steps, the basic longitudinal texture (BLT) was already found to be independent of the fracture toughness of composites [32,36]. All the other steps except debonded matrix and BLT are characterized in Fig. 1(B). First, the total length of steps per unit area (areal density) is measured using SEM micrographs, and using this data, the toughness increase by step formation through increasing actual fracture surface area is calculated and plotted against the average step height (Fig. 1(B)). Since the OM and SEM micrographs of fracture surface do not allow the step height to be precisely measured, the average step height is treated as a variable in a reasonable range, from 0 to 5 μm . Most SEM and OM micrographs show the step heights to be in this range. The toughness increase is calculated based on the G_{IC} of unmodified epoxies. As can be seen in the plot, the calculated toughness increase, r_{cal} , is

usually less than 1.1. However, the measured toughness increases due to the incorporation of glass beads, r_{exp} , are much larger than the calculated increases. In Fig. 1(B), the minimum measured value is 1.68, which is still much larger than the maximum calculated value. Consequently, it can be stated that the contribution of step formation to toughening by increasing actual fracture surface area is not substantial. The possible plastic deformation during the mixed mode fracture of step formation is also unlikely to be a significant mechanism. Although the contribution of plastic deformations is not considered in the calculation of the toughness increases, Fig. 1(B) provides this result by showing that the measured fracture toughness increases do not follow an increase in the areal density of steps. As a result, step formation can not be the dominant energy dissipating mechanism for glass bead filled epoxies.

3.2. Debonding of glass beads/diffuse matrix shear (DS) yielding

Debonding of glass beads and diffuse shear (DS) yielding of matrix are combined into one mechanism, because they were always found together in our previous studies [32–36]. The proposed formation mechanism is consistent with our experimental finding: Once a glass bead debonds from the matrix, matrix shear yielding can then occur around this surface region in a plane stress condition. The direct measurement of fracture energy dissipated through the debonding/DS yielding is currently impossible. Therefore, only a correlation study between the size of the debonding/DS yielding zone (debonding zone) and the fracture toughness of composites was conducted.

Several debonding zone sizes ($2r_{dc}$) measured by using OM and SEM are given in Fig. 2. Generally, as the glass bead content increases, the debonding zone size also increases. (The error range is the standard deviation of experimental data.) The cleaned glass bead system (LG/661) has a significantly smaller zone size than the other two systems at 10 vol% glass bead content. This may be reasonable, because our microscopy [32–36] showed that uncleaned and rubber encapsulated glass bead systems had lower interfacial strength than cleaned glass bead systems. Larger debonding zone sizes could result from lower interfacial strength, if K_{IC} is not significantly varied. However, the difference found at 10 vol% is not noticeable at 20 and 30 vol%, where the error ranges are comparable to the differences among the debonding zone sizes. As glass bead content increases, the overlap of stress fields around glass beads will make the situation even more complicated.

In Fig. 2, an interesting comparison can be made between debonding zone size and inter-particle separation, D_i , calculated by using this equation [2,3].

$$D_i = \frac{2D_p(1 - C_f)}{3C_f} \quad (2)$$

Compared to D_i , 10 vol% LG/661 has a relatively small

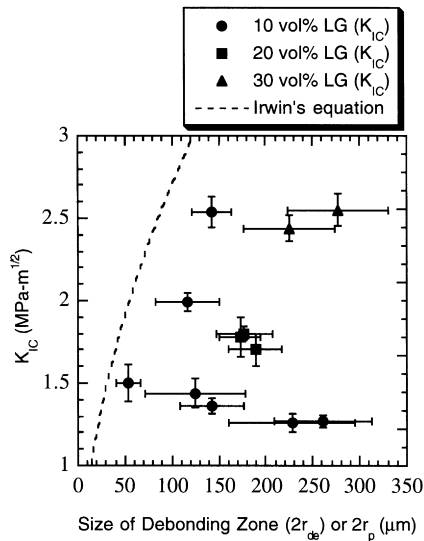


Fig. 3. Relationship between K_{IC} and debonding zone size ($2r_{de}$) for various glass bead filled epoxies. The dashed line is calculated from Irwin's theoretical relation, $K_{IC} = [3\pi(2r_p)]^{1/2}\sigma_y$, using σ_y (yield stress) of 661 epoxy resin (88 MPa), where r_p is the plastic zone size.

debonding zone size. On the other hand, u-LG or 0.5-LG systems have debonding zone sizes comparable to D_i at 10 vol%. In other words, the debonding zone of the former has only one array of glass beads and that of the latter has an average of two arrays of glass beads. For 20 and 30 vol%, 3–5 arrays of glass beads can exist inside the debonding zones.

Fig. 3 provides a plot of K_{IC} versus $2r_{de}$. For reference, the prediction of Irwin's theory [36] for plastic zone size ($2r_p$) under plane strain conditions is also presented. Since the debonding zone is not the plastic zone, the theoretical prediction is not necessarily consistent with the measured values of debonding zone size. The prediction shows a general trend instead: As plastic (or damage) zone size increases, K_{IC} increases. Fig. 3 clearly shows no correlation between K_{IC} and debonding zone size. In particular, the data of 10 vol% systems show too much scatter and no reasonable correlation in accordance with the general trend.

All data points in Fig. 3 can be categorized into three series of composites:

Series 1. Different Surface Treatments of Glass Beads—The five data points below $1.50 \text{ MPa m}^{1/2}$ of, from left to right in the plot, 10 vol% LG, u-LG, 0.5-LG, 1.5-LG, 3.0-LG filled epoxies,

Series 2. Different Inherent Matrix Toughness—10 vol% LG/661 ($54 \mu\text{m}$, $1.50 \text{ MPa m}^{1/2}$), 10 vol% LG/664 ($116 \mu\text{m}$, $1.99 \text{ MPa m}^{1/2}$), and 10 vol% LG/667 ($143 \mu\text{m}$, $2.54 \text{ MPa m}^{1/2}$),

Series 3. Different Volume Fraction of Glass Beads—20 and 30 vol% data with the data of 10 vol% LG, u-LG, 0.5-LG filled epoxies in series 1.

A reasonable relation similar to the theoretical prediction can be observed among the data points of series 2 and 3: K_{IC} increases with increasing debonding zone size. As inherent matrix toughness or glass bead content increases, debonding zone size increases, resulting in the increase of fracture toughness. On the other hand, the series 1 data show a different relation: K_{IC} is independent of debonding zone size. This result reveals that an increase of debonding zone size is not always followed by an increase of fracture toughness.

If a micro-mechanical deformation can dissipate a significant amount of fracture energy resulting in the increase of fracture toughness (ΔG_{IC}), ΔG_{IC} must scale with the size of this deformation zone (r_p). A simple relationship has been proposed as follows:

$$\Delta G_{IC} = \eta r_p \quad (3)$$

where η is a coefficient dependent on the characteristics of the micro-mechanical deformation [37–39]. (The direct proportionality of K_{IC}^2 to G_{IC} in our systems can be found elsewhere [32–36].) Accordingly, it is not the debonding/DS yielding mechanism that can dissipate the largest amount of fracture energy during the fracture of glass bead filled epoxies. There must be more dominant energy dissipating mechanism(s) other than debonding/DS yielding.

Three important differences between the debonding/DS yielding mechanism for glass bead filled epoxies and the cavitation/shear yielding mechanism [40–43] for rubber particle toughened epoxies need to be discussed to satisfactorily understand the results shown in Fig. 3. First, compared to the cavitation/shear yielding mechanism, the debonding/DS yielding mechanism does not occur over as much of the volume [32–35]. In rubber particle toughened systems, profuse matrix shear yielding is triggered by dense rubber particle cavitation. In glass bead filled systems, only glass beads along the crack propagation path usually debond and DS yielding follows the debonding over relatively small regions. Furthermore, since the glass beads used in this study were much larger than the common rubber particles used as tougheners, the surface area in plane stress condition generated by debonding will be relatively small. As a result, even in a debonding zone whose size is comparable to the typical cavitation/shear yielding zone size, the volume of material actively dissipating fracture energy does not seem to be large enough to significantly contribute to toughening.

Another difference is that, contrary to the cavitation process, debonding seldom produces complete interfacial failure around glass beads. The initiation of debonding usually occurs from defects at the pole regions of the interface. (The pole region refers to the interfacial region between glass beads and the matrix perpendicular to the direction of the far-field stress.) From the initiation sites, debonding will then spread out along the interface. As debonding progresses to the equatorial parts of glass beads, the stress needed to break the interface increases, as can be expected [44]. As discovered in the previous

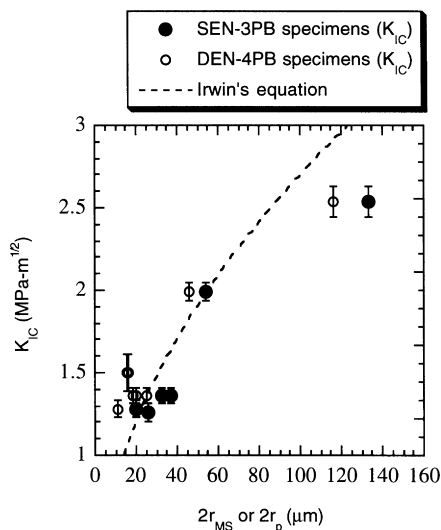


Fig. 4. Relationship between K_{IC} and micro-shear band zone size ($2r_{MS}$) measured for various 10 vol% glass bead filled epoxies. $2r_{MS}$ is $2(A_{MS}/\pi)^{1/2}$, where A_{MS} is the area of micro-shear band zone measured. The dashed line is calculated from Irwin's theoretical relation, $K_{IC} = [3\pi(2r_p)]^{1/2}\sigma_y$, using σ_y (yield stress) of 661 epoxy resin (88 MPa), where r_p is the plastic zone size.

SEM and OM microscopy studies [32–35], only half or less than half of the surface area of glass beads are usually debonded. Consequently, the volume fraction of microcracks in a debonding zone will be smaller than expected. Thus, this incomplete debonding could be less effective in triggering matrix shear yielding than the cavitation of rubber particles.

The last difference is the mismatch of coefficients of thermal expansion (CTE). In general, rubber particles have larger CTE than epoxy. Thus, during the preparation of rubber-toughened epoxies, tensile radial stresses and compressive hoop stresses are developed around rubber particles. This stress condition can help the cavitation process. In contrast, glass bead filled epoxies have an opposite situation. Since glass beads have smaller CTE than epoxy matrix, compressive radial stresses and tensile hoop stresses are developed around glass beads. This stress condition suppresses the debonding process, resulting in less extensive and less dense debonding/DS yielding.

From the analysis of thermal residual misfit stress around glass beads, it has been expected [27,28,45] that microcracking can occur in the matrix around glass beads initiating from the equatorial regions and propagating out in the radial direction. However, these annular microcracks isolated from the primary crack were not found in the SEM or OM micrographs of our previous studies [32–35]. Thus, what needs to be considered is not the role of thermal residual misfit in initiating annular microcracks but its suppression effect on debonding.

3.3. Micro-shear (MS) banding

As is the case in the study on debonding/DS yielding mechanism, since the direct measurement of energy dissipated by MS banding is not experimentally accessible, only a correlation study between fracture toughness and MS band zone size was conducted. Fig. 4 shows a plot of K_{IC} versus $2r_{MS}$ (equivalent diameter of MS band zone). $2r_{MS}$ is measured by using SEN-3PB and DEN-4PB specimens. The data obtained by using DEN-4PB specimens are usually smaller than those obtained by using SEN-3PB specimens. This is reasonable, because a crack in a DEN-4PB specimen is not yet critically loaded, so MS bands at the crack tip region are not fully developed yet.

Although the plastic zone ($2r_p$) in Irwin's theory [36] is not precisely the same as the MS band zone found in this experiment, the prediction of the theory shows very good agreement with the measured MS band zone sizes. This does not necessarily mean that Irwin's equation can be used to predict $2r_{MS}$; rather it indicates that the $2r_{MS}$ values may be large enough to allow the MS banding to dissipate a significant amount of fracture energy. The calculated values ($2r_p$) can be converted directly into the fracture energy of composites under a linear elastic condition [36].

Contrary to Figs. 3 and 4 shows a simple relationship between K_{IC} and $2r_{MS}$, which is similar to Eq. (3): K_{IC} increases with $2r_{MS}$, regardless of the surface treatments of glass beads and inherent matrix toughness. In particular, the scattered data set of series 1 in Fig. 3 are collapsed into a small region (around 20 μm , 1.3 $\text{MPa}\cdot\text{m}^{1/2}$) in Fig. 4. This collapsing result tells us that the change of interfacial strength according to the surface treatments could not affect both MS band zone size and the fracture toughness of composites. While the composites in series 1 prepared by different surface treatments have a similar MS band zone size and fracture toughness, their debonding zone sizes vary in a wide range. Thus, the fracture toughness can achieve a simple correlation with not debonding zone size but MS band zone size. This is a unique discovery. If the MS band zone size of a composite is known, the approximate fracture toughness of the composite can be estimated. Accordingly, MS banding must be the major source of toughness for glass bead filled epoxies.

It is worth mentioning that MS bands were not always found in all the glass bead filled epoxies prepared in our experiments. When 332 epoxy resin was used as a matrix, no MS bands were found in the process zone [32–35]. Therefore, it can be expected that the MS banding mechanism is not the major toughening mechanism in these more brittle matrix systems. However, the toughness increase found in 332 systems due to the incorporation of glass beads is much smaller than those found in other tough matrix systems [32–35]. The very small toughness increase can be attributed to the other mechanisms, e.g. debonding/DS yielding and step formation. If successful and significant toughening results from the use of glass beads in a

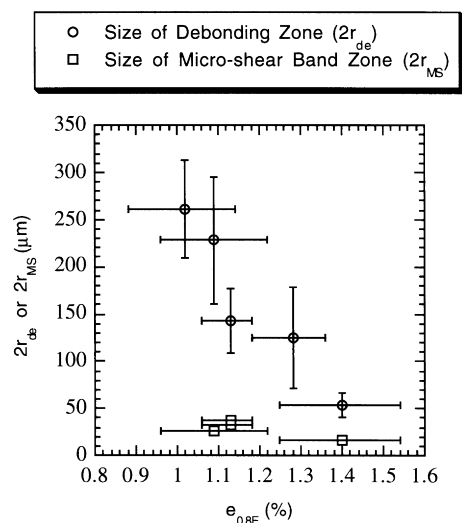


Fig. 5. Relationship between $e_{0.8E}$ and debonding zone size ($2r_{de}$) or micro-shear band zone size ($2r_{MS}$) measured for various 10 vol% glass bead filled epoxies. The $e_{0.8E}$ is the strain where tangential modulus drops to 80% of initial modulus during the uniaxial tensile test of glass bead filled epoxies.

composite system, MS banding is most likely to be the major toughening mechanism.

MS banding is thought to occur due to the strain softening behavior of materials and the existence of initial strain inhomogeneities [46–51]. If the characteristic strain of materials (ε^*) and the initial strain inhomogeneity ($\Delta\varepsilon$) are known, the critical strain to initiate MS banding (ε^c) can be calculated by the model proposed by Bowden [47]:

$$\varepsilon^c = \varepsilon^* \ln(\varepsilon^*/\Delta\varepsilon) \quad (4)$$

In glass bead filled epoxies, the existence of glass beads can provide large $\Delta\varepsilon$ values and the strain softening behavior of epoxies can provide favorable ε^* values for MS banding. Therefore, the existence of glass beads in the epoxy matrix is likely to facilitate MS deformation which is otherwise difficult to occur. MS bands initiate from the interface between glass beads and matrix ahead of crack tips, and then propagate through the matrix. A significant amount of energy can be absorbed during MS banding. The propagation of MS bands is not likely to be affected seriously by the debonding of glass beads. Once a glass bead debonds from the matrix, DS yielding around the debonded surface of matrix seems to be the favored mode of deformation. To confirm the initiation and propagation mechanism of MS bands proposed above, future studies are necessary.

3.4. Interfacial strength between glass beads and matrix

In inorganic particle filled polymers, the interfacial strength between inorganic particles and the matrix is an important material parameter. It has a significant effect on the various mechanical properties of materials (e.g. modulus, tensile strength, elongation to break, etc.). However, in

the current experiments and also the previous reports [2–6,52], the interfacial strength between the glass beads and epoxy matrix has not been found to significantly affect the fracture toughness of composites. Even silation and releasing agent treatments have not been found effective in improving the fracture toughness of the composites. These findings have never been explained successfully. The crack front bowing mechanism [5,8–11,14,15] cannot explain properly this effect either. Fortunately, the relationship between the fracture toughness and the size of micro-mechanical deformations is successfully established in this study. Therefore, if the relationship between the size of deformation zones and the interfacial strength can be established, the mystery is more likely to be solved.

For the correlation study, the absolute values or at least the relative degree of the interfacial strength between glass beads and matrix in various composites must be obtained. Measuring the absolute values does not seem possible. The relative degree of the interfacial strength can be qualitatively assessed by SEM microscopy studies [32–35]. However, this method is not really sensitive to changes of the interfacial strength. Thus, a new parameter, $e_{0.8E}$, is introduced as a measure of interfacial strength. $e_{0.8E}$ is the critical strain where tangential modulus drops to 80% of initial Young's modulus during uniaxial tensile testing of glass bead filled epoxies. It must depend on the load carrying capability of the glass beads, and in turn, this capability should depend on the area of debonded surface during loading. Consequently, $e_{0.8E}$ will depend on the interfacial strength between glass beads and the matrix. However, since the debonding is not a simple process, the $e_{0.8E}$ values cannot be easily converted into quantitative data on interfacial strength. Moreover, the size dependence of the critical stress for debonding [32,44] makes the situation more complicated. Therefore, $e_{0.8E}$ will be used simply as a relative measure of the interfacial strength.

The plot of MS band zone or debonding zone sizes versus $e_{0.8E}$ is given in Fig. 5. All the data in this plot belong to the series 1, whose interfacial strength is found to decrease in the following order: LG, u-LG, 0.5-LG, 1.5-LG, 3.0-LG systems. This is similar to our previous SEM results [32–35]. (The $e_{0.8E}$ values of glass bead filled epoxies were found to be smaller than that of unmodified epoxy.) Although not many data points are used in Fig. 5, it can be noticed that the debonding zone size is inversely proportional to the interfacial strength. As interfacial strength decreases, there are more debonded glass beads. On the other hand, the MS band zone size shows no relationship with the interfacial strength. These results are consistent with the proposed initiation mechanisms of MS banding and debonding/DS yielding. Since MS banding is found to be the major energy dissipating mechanism and does not significantly depend on the interfacial strength, the interfacial strength cannot significantly affect the fracture toughness of composites.

Before the $e_{0.8E}$ measurements, tensile dilatometry was carried out to evaluate the interfacial strength using the

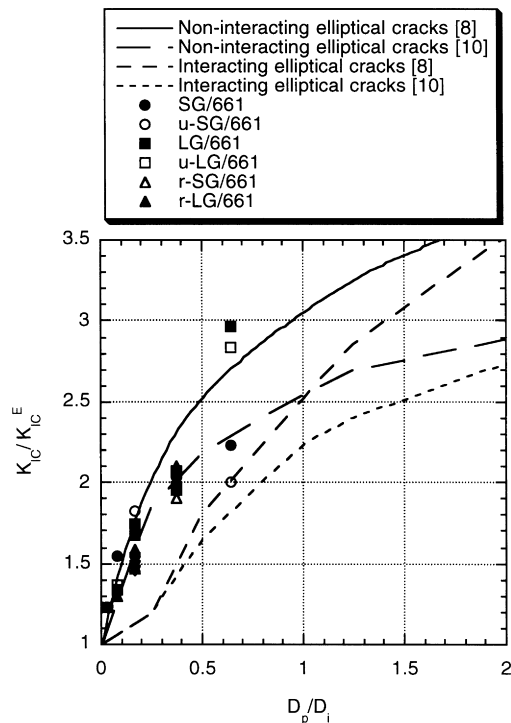


Fig. 6. K_{IC}/K_{IC}^E from experiments and theoretical predictions versus D_p/D_i for glass bead filled epoxies. K_{IC} and K_{IC}^E is the critical stress intensity factor of glass bead filled and unmodified epoxy resins, respectively. D_p is the diameter of glass beads and D_i is inter-particle distance.

same experimental techniques reported by Yee and Pearson [40]. However, this method was found to be less sensitive than $e_{0.8E}$ measurement. Meddad and Fisa also showed the same sensitivity problem of tensile dilatometry in their study on glass bead filled thermoplastics [53].

3.5. On crack front bowing mechanism

Among the micro-mechanical deformations, MS banding was established as the major toughening mechanism for glass bead filled epoxies. A question is then raised: Is the crack front bowing mechanism wrong? This mechanism could not explain the effect of various material variables, such as the interfacial strength.

The predictions of fracture toughness based on the crack front bowing mechanism were found to be roughly consistent with experimental values. The experimental data of the current research roughly follow the predictions as well. An example is given in Fig. 6. The predictions of four different theoretical approaches are compared with our experimental data. The experimental data show a reasonably good agreement with the increase of fracture toughness (K_{IC}/K_{IC}^E) calculated by using the two equations for non-interacting elliptical cracks.

Although the predictions of the crack front bowing theory approximate the experimental data, the variation of the experimental K_{IC}/K_{IC}^E values in Fig. 6 cannot be explained by using this theory. For example, at $D_i/D_p = 0.64$ in Fig. 6,

K_{IC}/K_{IC}^E varies from 2.0 to 2.97. This variation comes from changes in material parameters (e.g. size of glass beads, inherent matrix toughness, surface treatments). The crack front bowing theory cannot relate this variation to the change of material parameters. The different assumptions in the theoretical approaches regarding non-interacting or interacting and elliptical or circular cracks are related with neither material parameters nor experimental findings. The shape of commonly observed secondary crack fronts at break-away positions is neither elliptical nor circular [9–11]. Furthermore, it seems to be independent of most material parameters [9–11].

The fundamental limitation of the crack front bowing theory comes from its assumption that there is a certain degree of resistance (impenetrability) of particles against crack propagation. This theory does not identify the source of the resistance. Consequently, this theory can hardly be connected with material parameters.

In fact, the basic concept of crack front bowing theory is valid and the crack front bowing between particles is indeed found to occur in the fracture of glass bead filled epoxies. However, it mainly focuses on the relation between particle's resistance against crack propagation and the fracture toughness of composites rather than the origin of the resistance. The current approach aimed at a more fundamental level can give more details of the toughening mechanism for glass bead filled epoxies.

In this study, only glass bead filled epoxies were used as the model systems of inorganic particle toughening. To generalize the results for understanding other inorganic particle toughened systems; more studies on the fundamental sources of toughness similar to this study are necessary.

4. Conclusions

The major energy dissipating mechanism for glass bead filled epoxies was determined. Unlike the crack front bowing mechanism, it is related to material properties and parameters. This was done by studying correlation between the size of micro-mechanical deformation zone and fracture toughness of materials. If a micro-mechanical deformation could dissipate a dominant amount of fracture energy, fracture toughness should increase in proportional to the size of the deformation. Three kinds of micro-mechanical deformations occurring in the fracture of glass bead filled epoxies were investigated, i.e. (1) step formation; (2) debonding of glass beads/DS yielding of matrix; and (3) MS banding.

Among the micro-mechanical deformations, step formation and debonding/DS yielding were identified as secondary-toughening mechanisms for glass bead filled epoxies. The areal density of steps was varied by changes in the volume content and size of glass beads and also inherent matrix toughness. However, the fracture toughness of composites was shown to be independent of changes in step formations. Furthermore, the estimated contribution

of step formation to toughening was found to be insignificant. The combined process, debonding/DS yielding, was found to become more noticeable as inherent matrix toughness and glass bead content increased. However, a reasonable correlation between the fracture toughness of composites and the size of this deformation zone could not be obtained.

Contrary to the other two micro-mechanical deformations, MS banding showed a simple and reasonable correlation between the size of MS band zone with the fracture toughness of composites. Furthermore, the size was found to be large enough to dissipate a significant amount of fracture energy. Therefore, MS banding was proposed as the major source of toughness for glass bead filled epoxies. If the size of MS band zone was known, the fracture toughness could be estimated. The role of glass beads as stress concentrators and the strain-softening characteristic of matrix were thought to facilitate the MS banding. It was proposed that MS banding initiated at the interface between glass beads and matrix where strain inhomogeneity was a maximum, and propagated into the matrix in radial directions from the glass beads. This proposed mechanism was consistent with the experimental finding that there was no simple relationship between the interfacial strength and the size of MS band zone. As a consequence, the previous experimental results, i.e. that the fracture toughness of glass bead filled epoxies does not depend on the surface treatments of glass beads, could be explained successfully by using the major toughening mechanism.

Acknowledgements

This work was supported by the Specialized Materials Science Research Center of National Institute of Health (NIH), under a contract No. DEO 9296-09. Authors would like to thank Dr Jimmy Kishi and Dr Jack Huang for their help.

References

- [1] Rothon R. Particulate-filled polymer composites. Longman Scientific and Technical, 1995.
- [2] Spanoudakis J, Young RJ. *J Mater Sci* 1984;19:473.
- [3] Spanoudakis J, Young RJ. *J Mater Sci* 1984;19:487.
- [4] Moloney AC, Kausch HH, Stieger HR. *J Mater Sci* 1983;18:208.
- [5] Lange FF, Radford KC. *J Mater Sci* 1971;6:1197.
- [6] Broutman LJ, Shau S. *Mater Sci Engng* 1971;8:98.
- [7] Young RJ, Beaumont PWR. *J Mater Sci* 1977;12:684.
- [8] Lange FF. *Philos Mag* 1970;22:983.
- [9] Green DJ, Nicholson PS, Embury JD. *J Mater Sci* 1977;12:987.
- [10] Green DJ, Nicholson PS, Embury JD. *J Mater Sci* 1979;14:1413.
- [11] Green DJ, Nicholson PS, Embury JD. *J Mater Sci* 1979;14:1657.
- [12] Lange FF. *J Am Ceram Soc* 1971;54:614.
- [13] Lange FF. *J Am Ceram Soc* 1973;56:445.
- [14] Evans AG. *Philos Mag* 1972;26:1327.
- [15] Gao H, Rice JR. *Int J. Fract* 1987;33:155.
- [16] Rice JR, Ben-Zion Y, Kim K. *J Mech Phys Solids* 1994;42:813.
- [17] Perrin G, Rice JR. *J Mech Phys Solids* 1994;42:1047.
- [18] Rose LRF. *Mech Mater* 1987;6:11.
- [19] Brown SK. *Br Polym J* 1980:24.
- [20] Nakamura Y, Yamaguchi M, Okubo M, Matsumoto T. *Polymer* 1991;32:2221.
- [21] Nakamura Y, Yamaguchi M, Okubo M, Matsumoto T. *Polymer* 1991;32:2976.
- [22] Nakamura Y, Yamaguchi M, Okubo M, Matsumoto T. *Polymer* 1992;33:3415.
- [23] Nakamura Y, Yamaguchi M, Okubo M, Matsumoto T. *J Appl Polym Sci* 1992;44:151.
- [24] Nakamura Y, Yamaguchi M, Okubo M, Matsumoto T. *J Appl Polym Sci* 1992;45:1281.
- [25] Nakamura Y, Yamaguchi M, Okubo M. *Polym Engng Sci* 1993;33:279.
- [26] Faber KT, Evans AG. *Acta Metall* 1983;31:565.
- [27] Azimi HR, Pearson RA, Hertzberg RW. *Polym Engng Sci* 1996;36:2352.
- [28] Evans AG, Williams S, Beaumont PWR. *J Mater Sci* 1985;20:3668.
- [29] Evans AG, Fu Y. *Acta Metall* 1985;33:1525.
- [30] Rose LRF. *J Am Ceram Soc* 1986;69:212.
- [31] Hutchinson JW. *Acta Metall* 1987;35:1605.
- [32] Lee J., Ph.D. Thesis, The University of Michigan, 1998.
- [33] Lee J, Yee AF. *Polym Prepr (Am Chem Soc, Div Polym Chem)* 1997;38:369.
- [34] Lee J, Yee AF. *Polym Prepr (Am Chem Soc Div Polym Mater)* 1998;79:200.
- [35] Lee J, Yee AF. *Polymer* 2000 (in press).
- [36] Williams JG. *Fracture mechanics of polymers*. 1st ed. Chichester, UK: Ellis Horwood, 1984.
- [37] Evans AG, Ahmad ZB, Gilbert DG, Beaumont PWR. *Acta Metall* 1986;34:79.
- [38] McMeeking RM, Evans AG. *J Am Ceram Soc* 1980;63:240.
- [39] Budiansky B, Hutchinson J, Lambropoulos J, *Int J. Solids Struct* 1983;19:337.
- [40] Yee AF, Pearson RA. *J Mater Sci* 1986;21:2462.
- [41] Pearson RA, Yee AF. *J Mater Sci* 1986;21:2475.
- [42] Yee AF, Li D, Li X. *J Mater Sci* 1993;28:6392.
- [43] Li D, Yee AF, Chen IW, Chang SC, Takahashi K. *J Mater Sci* 1994;29:2205.
- [44] Gent AN. *J Mater Sci* 1980;15:2884.
- [45] Koh S, Kim J, Mai Y. *Polymer* 1993;34:3446.
- [46] Argon AS, Andrews RD, Godrick JA, Whitney W. *J Appl Phys* 1968;39:1899.
- [47] Bowden PB. *Philos Mag* 1970;25:455.
- [48] Bowden PB, Raha S. *Philos Mag* 1970;25:463.
- [49] Kramer EJ. *J Polym Sci, Polym Phys Ed* 1975;13:509.
- [50] Wu JBC, Li JBC. *J Mater Sci* 1976;11:434.
- [51] Li JBC, Wu JBC. *J Mater Sci* 1976;11:445.
- [52] Sahu S, Broutman LJ. *Polym Engng Sci* 1972;12:91.
- [53] Meddad A, Fisa B. *J Appl Polym Sci* 1997;64:653.